

Statistical Exploration of Fragmentation Phase Space and Source Sizes in Nuclear Multifragmentation

L. G. Moretto, L. Beaulieu*, L. Phair, and G. J. Wozniak

Nuclear Science Division, Lawrence Berkeley National Laboratory, Berkeley, California 94720

(November 21, 2018)

Abstract

The multiplicity distributions for individual fragment Z values in nuclear multifragmentation are binomial. The extracted maximum value of the multiplicity, m_Z , is found to depend on Z according to $m_Z = Z_0/Z$, where Z_0 is the source size. This is shown to be a strong indication of statistical coverage of fragmentation phase space. The inferred source sizes coincide with those extracted from the analysis of fixed multiplicity charge distributions.

arXiv:nucl-ex/9812010v2 15 Feb 2000

Is nuclear multifragmentation [1,2] a statistical or a dynamical process? Let us consider a fragmentation space defining the number and masses/charges of the produced fragments. The thermal population of each cell can be expressed in terms of suitable Boltzmann factors. The thermal nature of this population can be tested in a variety of ways. A very visual way is the Arrhenius plot where the log of the population is plotted vs. the reciprocal temperature $1/T$.

The question however, remains whether, apart from the Boltzmann factor, all the cells of the fragmentation space are uniformly explored. A test of such a uniform filling implies the knowledge of the size (mass/charge) of the source. A new empirical feature observed in many reactions has led us to a way to verify the uniform filling of fragmentation space and to determine simultaneously the source size.

It has been shown [3] that the intermediate mass fragment (IMF) multiplicity distribution P_n at any given transverse energy E_t is *empirically* given by a binomial distribution

$$P_n = \frac{m!}{n!(m-n)!} p^n (1-p)^{m-n}. \quad (1)$$

This implies that fragments are emitted nearly independently of each other, so that the probability P_n of observing n fragments can be written by combining a single one-fragment emission probability p according to Eq. (1). The parameter m (the total number of throws) represents the maximum possible number of fragments, which is immediately related to the source size.

The simplest statistical equilibrium model of multifragmentation has exactly the structure of Eq. (1). Let us assume that the source is made up of m fragments. The “outside” fragments have energy ϵ_2 , and those “inside” have energy ϵ_1 . A generic partition of n fragments outside and $m-n$ fragments inside has the probability:

$$P_n = \frac{m!}{n!(m-n)!} \frac{e^{-(n\epsilon_2+(m-n)\epsilon_1)/T}}{(e^{-\epsilon_1/T} + e^{-\epsilon_2/T})^m} \quad (2)$$

which leads to Eq. (1) when

$$p = \frac{e^{-\epsilon_2/T}}{e^{-\epsilon_1/T} + e^{-\epsilon_2/T}}. \quad (3)$$

Thus, a simple way to obtain the size of the source is to multiply m by the fragment size.

When the definition of IMF covers a range of atomic numbers (IMF: $Z_{th} \leq Z \leq 20$, with Z_{th} equal to 3), one should multiply m by a “suitably” averaged Z . In fact, a dependence of m on the lower threshold Z_{th} has been found such that $m(Z_{th}) \times Z_{th} \approx \text{constant}$ [3]. The natural next step is to restrict the fragment definition to a single atomic number Z .

A straightforward generalization of Eq. (1) to the production of fragments with charges 1, 2, ... Z_0 is given by the multinomial distribution

$$P = \frac{Z_0!}{n_1!n_2!\dots n_{Z_0}!} p_1^{n_1} p_2^{n_2} \dots p_{Z_0}^{n_{Z_0}} \quad (4)$$

with

$$Z_0 = \sum_Z Z n_Z. \quad (5)$$

Here there is no single quantity m as in Eq. (1), since the constraint is now on the total charge rather than on the total number of fragments. However, this leads immediately to a simple scaling that must be obeyed if the fragmentation phase space is to be completely explored.

Let us first consider, as a familiar example, the fragmentation space spanned by the Euler number partitions. This case is particularly simple because all partitions are unbiased, or equally probable. This would correspond, for the different model defined in Eqs. (4) and (5), to setting $p_i = \text{constant}$.

Let us indicate with $W(Z_0)$ the statistical weight (number of partitions) associated with the integer or “charge” Z_0 . If we now select the partitions containing at least n_Z integers of size Z , their number is given by the number of partitions of the residue

$$P_{n_Z} = W(Z_0 - n_Z Z) \quad (6)$$

by definition. Since the “charge” constraint is applied “minimally,” what counts is only the product $Z n_Z$, rather than the individual Z values. Consequently, the weight of the residue does not change if we substitute $n_Z Z$ with $n_{Z'} Z'$ provided that $n_Z Z = n_{Z'} Z'$. In other words, $P_{n_Z, Z} = P_{n_{Z'}, Z'}$ if $n_Z Z = n_{Z'} Z'$.

This gives immediately the scaling laws

$$n_Z/n_{Z'} = Z'/Z \quad (7)$$

or for the extreme value of $n_Z = m_Z$,

$$m_Z = Z_0/Z. \quad (8)$$

This result follows directly from the uniform exploration of the fragmentation phase space. It amounts to a *complete decoupling* of all the fragmentation paths. Once the system attains the charge loss of $q = nZ$, it is indifferent to how this was attained. *Any* path $q = \sum n_i Z_i$ is *equivalent* and *substitutable*. Similarly, for the remaining charge $Z_0 - q$.

This argument works when all partitions are unbiased, as for instance in the Euler number partition mentioned above. However, in the binomial/multinomial distributions of Eqs. (1) and (4), each partition is weighted by the probabilities p_i (reflecting Q -value effects) which may or may not be Boltzmann factors.

Yet, the binomial/multinomial analysis elegantly and automatically separates out the Q -value dependent probability p from the parameter m_Z which now contains direct information on the accessible fragmentation space and must follow the scaling given by Eq. (8). Thus the $1/Z$ scaling is the counterpart of the Arrhenius plot which verifies the thermal (Canonical) population of each fragmentation configuration.

When the restriction to *individual* Z values is made experimentally [4], the multiplicity distributions are found to be nearly Poissonian, namely $mp \ll m$. This introduces interesting simplifications in the analysis and interpretation of the data, but at the cost of a loss of scale. In the Poisson limit the average multiplicity $\langle n \rangle = mp$ is the only accessible parameter, and the decomposition into m and p becomes impossible. The recovery of scale for an individual Z is highly desirable in view of the possibility that the number of throws m_Z (for a single species Z) might obey the simple scaling of Eq. (8).

Thus, we have attempted binomial fits of the multiplicity distributions for *individual* Z values in an effort to extract m_Z . Fortunately, a number of reactions ($^{36}\text{Ar} + ^{197}\text{Au}$ at

35 to 110 AMeV [5], $^{129}\text{Xe}+^{27}\text{Al},^{51}\text{V},^{\text{nat}}\text{Cu},^{89}\text{Y}$, at 50 AMeV [6], and $^{129}\text{Xe}+^{197}\text{Au}$ at 50 to 60 AMeV [7]) have been studied with good Z resolution and high statistics. We first consider the asymmetric, intermediate-energy reactions in reverse kinematics exemplified by $^{129}\text{Xe}+^{\text{nat}}\text{Cu}$ at 50 AMeV, for which we can expect a single dominant fragment source.

Examples of both binomial and Poisson fits to the carbon yield from this reaction are shown in panel a) of Fig. 1. An improvement of the fit by using the binomial expression is observed for large fold numbers. A similar improvement is observed for each Z in all reactions listed in this letter.

The E_t dependence of the parameters m_Z from the binomial fits to the multiplicity distributions associated with each fragment atomic number leads to several observations. For each Z value, m_Z increases to a near constant value with increasing E_t . We approximate this behavior with the form $m_Z = m_Z^0 \tanh fE_t$. The parameter m_Z^0 represents the saturation value of m_Z for large E_t and f controls the rise of m_Z with increasing E_t . The solid lines in panel b) of Fig. 1 are the empirical fits to m_Z values extracted for lithium and oxygen emission from the reaction $^{129}\text{Xe}+^{\text{nat}}\text{Cu}$ at 50 AMeV. The other discontinuous lines are fits to data not shown ($Z=4-7$).

Furthermore, at all E_t values there is an overall decrease of m_Z with increasing fragment Z value in agreement with the expected scaling $Zm_Z = Z_0$. This remarkable dependence is exemplified in panel c) of Fig. 1 and in Fig. 2. By applying the expected scaling (Zm_Z), all of the fits to the $^{129}\text{Xe}+^{\text{nat}}\text{Cu}$ data collapse together, resulting in the approximate source “size” as a function of E_t . A weighted average ($\langle Z_0 \rangle$) of the data over different exit channels, constructed according to

$$\langle Z_0 \rangle (E_t) = \sum_Z Zm_Z(E_t)a_Z, \quad (9)$$

is shown by the symbols in panel c) of Fig. 1. The weight a_Z is the standard weight (proportional to the inverse square of the individual errors). A similar behavior is observed in two additional asymmetric reactions $^{129}\text{Xe}+^{51}\text{V}$ and ^{89}Y (see Fig. 1d).

The E_t dependence of the source size is tantalizing. The source size increases quickly

to a saturation value. The fact that E_t is related to impact parameter as well as to the total excitation energy may explain the observed features. In the highly asymmetric reverse kinematic reactions one quickly achieves sufficient overlap to produce a dominant Xe-like source as one moves from peripheral to central collisions.

As a special case of the $1/Z$ scaling, the “saturation” m_Z values from central collisions of the reverse kinematics reactions (the top 5% of the E_t scale, shown by the hatched regions in panel b) of Fig. 1), are shown in Fig. 2. The open symbols represent the scaled quantity $Zm_Z = Z_0$. The solid lines are weighted averages for the different reactions. The same data in the form m_Z/Z_0 vs. Z are shown by the solid symbols, where the $1/Z$ dependence is manifested by the good agreement of the data with the values of $1/Z$ (solid line). This striking $1/Z$ dependence of the parameter m_Z is observed for all asymmetric systems measured.

These overall results for asymmetric reactions suggest the dominance of a single source, *strongly support the hypothesis of uniform (statistical) exploration of the fragmentation phase space*, and lead to the interpretation of $Z_0 = Zm_Z$ as the source “size.” The $1/Z$ scaling is general and should be observed in models used to describe multifragmentation.

In the less asymmetric reactions $^{129}\text{Xe}+^{197}\text{Au}$ at 50 and 60 AMeV for which at least two sources are plausible, we shall refer directly to $Z_0 = Zm_Z$ as the source size, although we shall see that now it depends on the fragment Z value as well as on E_t . The weak decrease of the source size with increasing fragment size Z , already observable in $^{129}\text{Xe}+^{89}\text{Y}$ (Fig. 2), becomes more visible in the case of the ^{197}Au target. At low fragment Z values, the source size Z_0 is ≈ 70 and it decreases monotonically with increasing fragment size Z to a source size Z_0 of approximately 40-50. This fragment size dependence seems to suggest that for the ^{89}Y target and, most of all, for the ^{197}Au target there may be a distribution of sizes, the higher Z fragments being emitted preferentially by the smaller source(s).

The reactions $^{36}\text{Ar}+^{197}\text{Au}$ at 35, 50, 80, 110 AMeV give a picture intermediate between the $^{129}\text{Xe}+^{197}\text{Au}$ and the ^{129}Xe induced reverse kinematics reactions. They also give information of the source size dependence on bombarding energy. The source size at low fragment

Z increases from $Z_0 \approx 30$ to $Z_0 \approx 60$ as the bombarding energy increases, AMeV, while at higher fragment Z the source size increases from $Z_0 \approx 20$ to $Z_0 \approx 40$.

In previous work [8], it was empirically shown that the observed charge distributions resulting from nuclear multifragmentation obey the following invariant form:

$$P_n(Z) \propto \exp\left(-\frac{B(Z)}{\sqrt{E_t}} - cnZ\right) \quad (10)$$

where n is the total intermediate mass fragment multiplicity of the event; E_t is the total transverse energy; and $B(Z)$ is the ‘‘barrier’’ distribution.

From thermodynamic considerations and percolation simulations, it was shown that c in Eq. (10) vanishes when the gas of IMFs is in equilibrium with a liquid (residue source, or percolating cluster), and assumes a value $\propto 1/Z_0$ (Z_0 being the source size) when the source is wholly vaporized [3,8,9].

Experimentally, the parameter c undergoes an evolution with (transverse) energy from approximately zero to a positive constant [9]. Thus the source size evolves from near infinity (an ‘‘infinite’’ reservoir of fragments) to the actual size of the source. With the exception of the reactions $^{129}\text{Xe}+^{27}\text{Al}$, ^{51}V , Cu, ^{89}Y , this limit is attained. Thus, it is possible to plot the value of Z_0 determined from m_Z against that obtained from the c parameter (both for the top 5% most central collisions in E_t).

Such a plot is shown in Fig. 4. The result is striking. Not only are the two quantities well correlated, but they also agree quite well in absolute value. This good agreement gives confidence that we have gained direct access to the source size. This source (sources) is specifically the entity that generates the fragments through ‘‘chemical equilibrium’’. It does not contain the pre-equilibrium part which is often incorporated in other source reconstruction methods.

In conclusion, we have shown that: a) the binomial (nearly Poissonian) multiplicity distributions for individual fragment atomic numbers permit the extraction of the parameter m_Z , the number of throws; b) m_Z for reactions where a single source is clearly dominant has the form $m_Z = Z_0/Z$; c) the $1/Z$ dependence is dramatic proof that the fragmentation

phase space is statistically explored; d) source size(s) can be extracted and should reflect the region(s) where chemical (as opposed to physical) equilibrium is achieved; e) these source sizes agree with the sizes obtained from the analysis of multiplicity selected charge distributions in the E_t range where a single gas phase, or thermodynamic bivariate, prevails.

Acknowledgments

This work was supported by the Nuclear Physics Division of the US Department of Energy, under contract DE-AC03-76SF00098. One of us (L.B) acknowledges a fellowship from the National Sciences and Engineering Research Council (NSERC), Canada.

* Present address: Indiana University Cyclotron Facility, 2401 Milo B. Sampson Ln, Bloomington, IN 47408

REFERENCES

- [1] L. G. Moretto and G. J. Wozniak, *Annu. Rev. Nucl. & Part. Sci.* **43**, 379 (1993).
- [2] J. P. Bondorf *et al.*, *Phys. Rep.* **257**, 133 (1995).
- [3] L. G. Moretto *et al.*, *Phys. Rep.* **287**, 249 (1997).
- [4] L. Beaulieu *et al.*, *Phys. Rev. Lett.* **81**, 770 (1998).
- [5] R. T. Desouza *et al.*, *Phys. Lett. B* **268**, 6 (1991).
- [6] D. R. Bowman *et al.*, *Phys. Rev. C* **46**, 1834 (1992).
- [7] K. Tso *et al.*, *Phys. Lett. B* **361**, 25 (1995).
- [8] L. Phair *et al.*, *Phys. Rev. Lett.* **75**, 213 (1995).
- [9] L. G. Moretto *et al.*, *Phys. Rev. Lett.* **76**, 372 (1996).

FIGURES

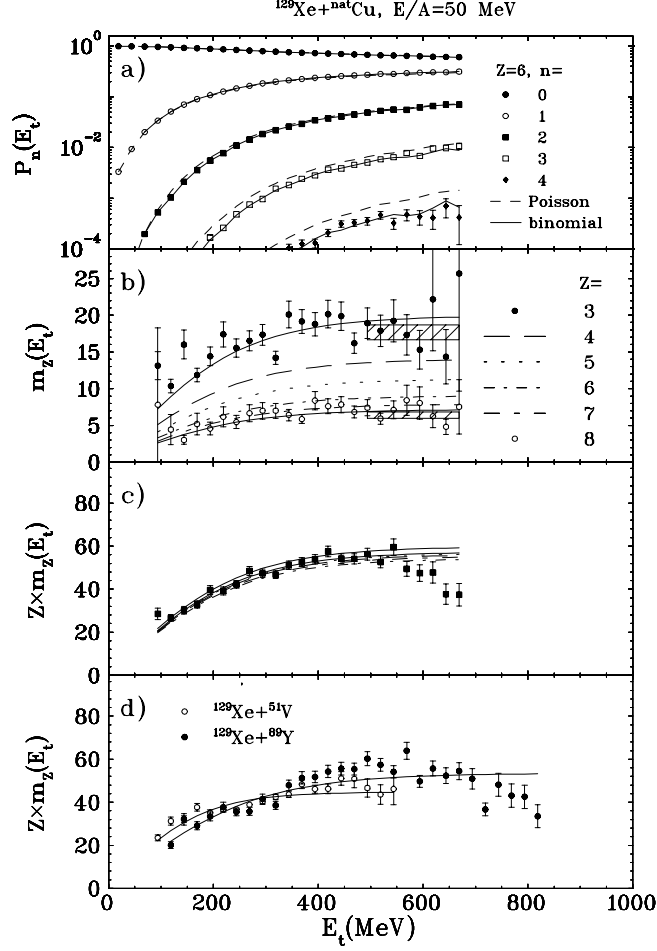


FIG. 1. Panel a): the n -fold probability distribution (symbols) and Poisson (dashed) and binomial (solid) fits are plotted as a function of transverse energy for carbon fragments emitted from the reaction $^{129}\text{Xe} + \text{natCu}$ at 50 AMeV. Panel b): the extracted binomial parameter m_Z (the number of “throws”) is plotted as a function of transverse energy for lithium (solid circles) and oxygen (open circles) emission. The solid lines are hyperbolic tangent fits to the indicated data. The other lines are fits to data not shown. The two hatched regions represent weighted averages of the top 5% most central collisions (based on the integrated E_t spectrum) of the m_Z values for lithium and oxygen. Panel c): The fits from panel b) are scaled by the atomic number Z of the emitted particle. The square symbols represent an “average” source size calculated with Eq. (9). Panel d): The symbols represent an “average” source size calculated with Eq. (9) for $^{129}\text{Xe} + ^{51}\text{V}$ and $^{129}\text{Xe} + ^{89}\text{Y}$. The lines are hyperbolic tangent fits to the data.

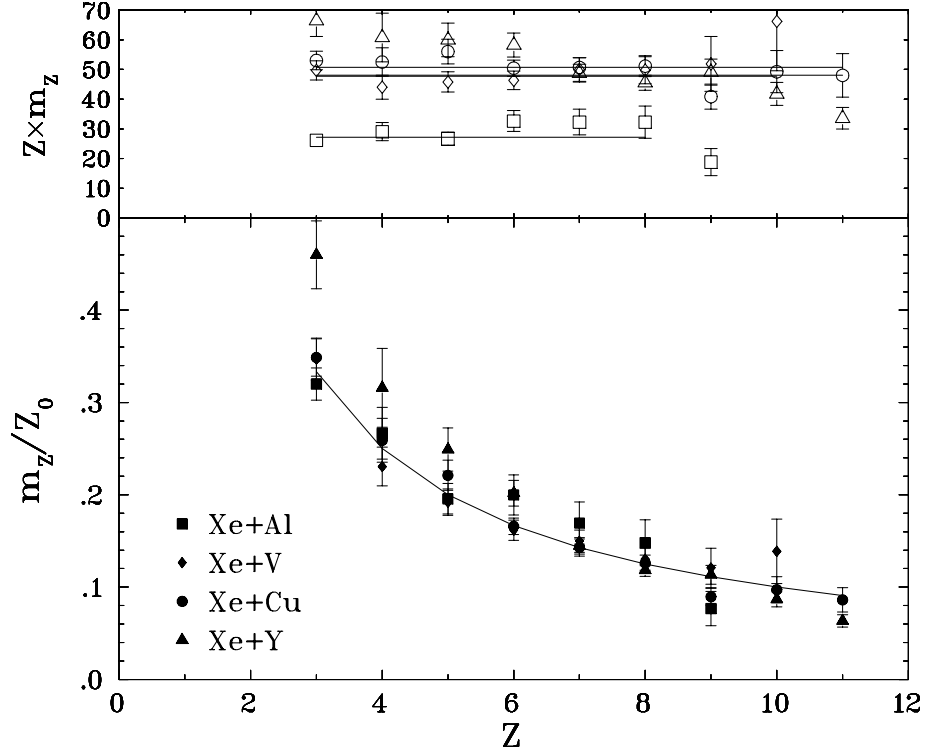


FIG. 2. Top panel: The m_Z values scaled by Z as a function of Z for the indicated reactions (open symbols) at 50 A MeV extracted for the 5% most central collisions. Bottom panel: The values of m_Z divided by the value of the extracted source charge Z_0 for the indicated reactions (solid symbols). The solid line is $1/Z$.

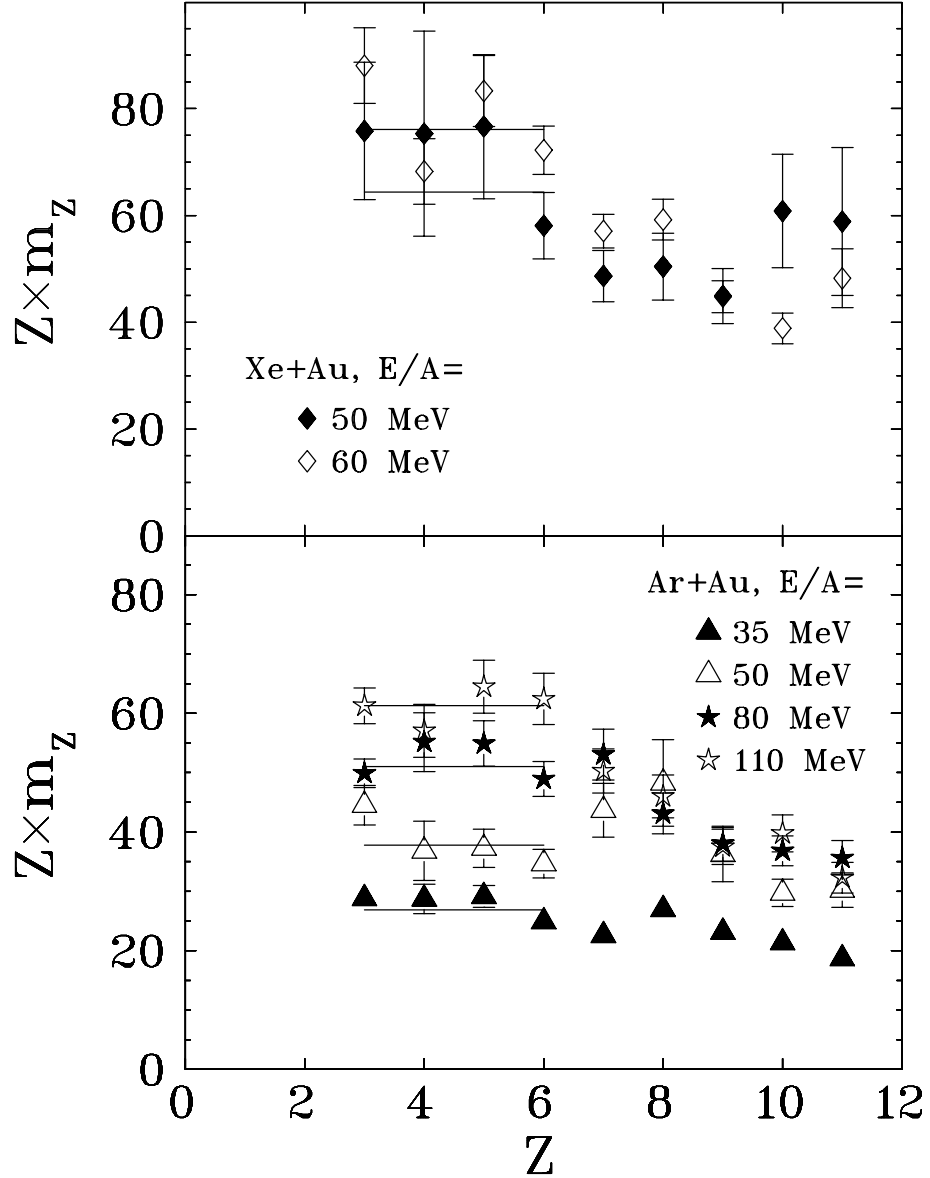


FIG. 3. The scaled values $Z \times m_Z$ are plotted for the indicated reactions of the 5% most central collisions. The solid lines represent weighted averages from $Z = 3$ to 6.

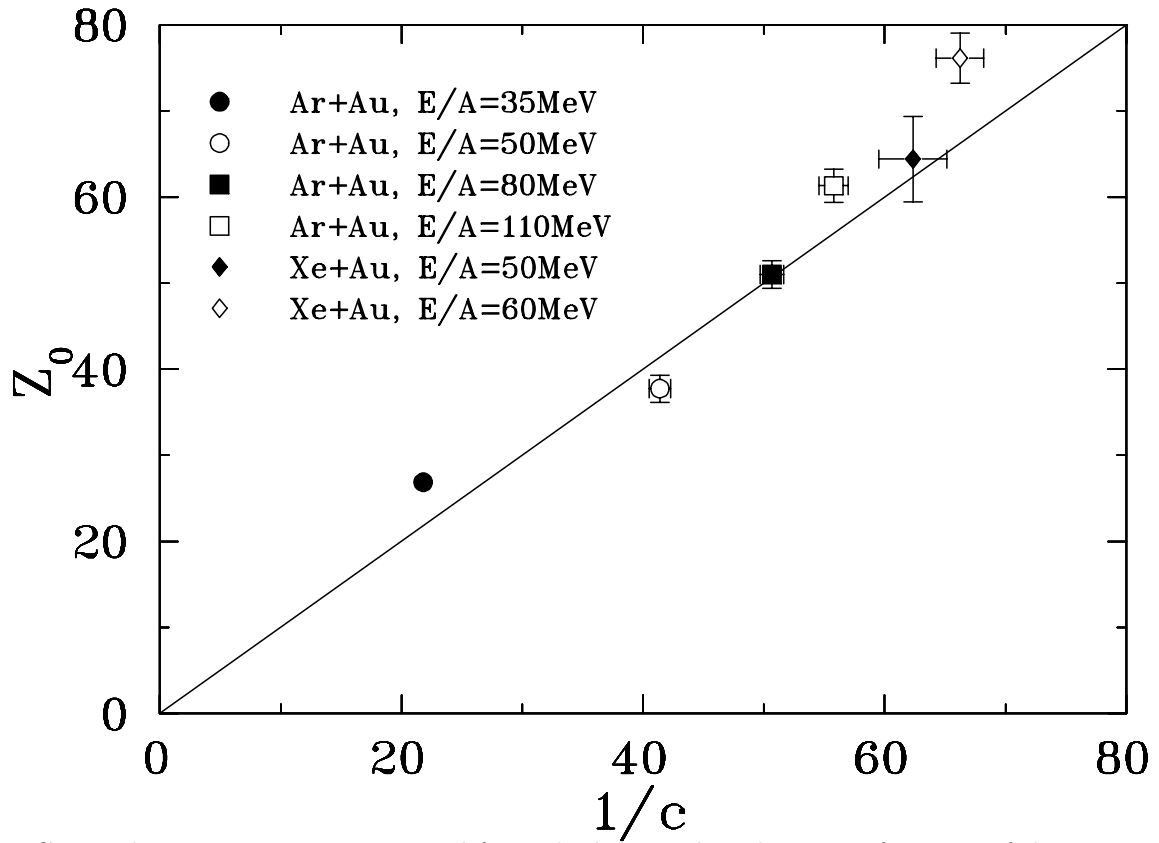


FIG. 4. The source size Z_0 extracted from the binomial analysis as a function of the source size ($1/c$) determined as per ref. [8] from central collision of the indicated reactions.